

EXPERIMENTAL MEASUREMENTS OF SLIPSTREAM DEFORMATION FOR AN INSTALLED DISTRIBUTED PROPELLER CONFIGURATION.

R.R. Duivenvoorden, F. do Nascimento Monteiro & T. Sinnige

Delft University of Technology, Delft, 2629HS, The Netherlands

Abstract

The integration of distributed electric propeller systems on aircraft wings presents complex aerodynamic interactions that are not yet fully understood. This study investigates the slipstream deformation in a distributed propeller configuration and compares it with a single propeller setup, visualised by experimental measurements of total pressure in the wake. Furthermore, we investigate the effects of relative blade phase angle on the resulting deformation. Overall, we identify several phenomena in distributed propeller-wing aerodynamic interaction that warrant attention in future research.

Keywords: distributed propellers, propeller-wing interaction, high-lift, slipstream deformation, experimental measurements

1. Introduction

The advancement of electric aircraft technology enables innovative propeller integration, such as Leading-Edge Distributed Propellers (LEDP) and active high-lift augmentation [1]. However, such propeller configurations feature complex aerodynamic interactions, both between propellers and with the wing, that are not fully understood.

De Vries et al. [2] show that interaction between adjacent propeller slipstreams is limited when no wing is present. While there is some dependency on the relative phase angle between the propellers, the system behaves mostly in a superpositional manner. This interaction dynamic is expected to change, however, when these slipstreams encounter a downstream wing. Previous studies on propeller-wing interaction, such as those by Samuelsson [3] and Veldhuis [4], show that the propeller slipstream deforms upon interaction with the wing. In cruise conditions, this deformation is primarily a spanwise shearing effect. In high-lift conditions, however, the slipstream deforms completely from its circular shape and expands significantly in spanwise direction [5, 6]. In a distributed propeller configuration, the proximity of adjacent slipstreams would restrict their deformation, as illustrated in Fig. 1, necessitating interaction as they pass the wing. This can be seen in several recent numerical studies on the topic, such as in the work by Keller [7], shown in Fig. 2. However, it has never been the focus of analysis in literature. Furthermore, there is little to no experimental data on the off-the-surface flow of distributed propeller configurations available in literature.

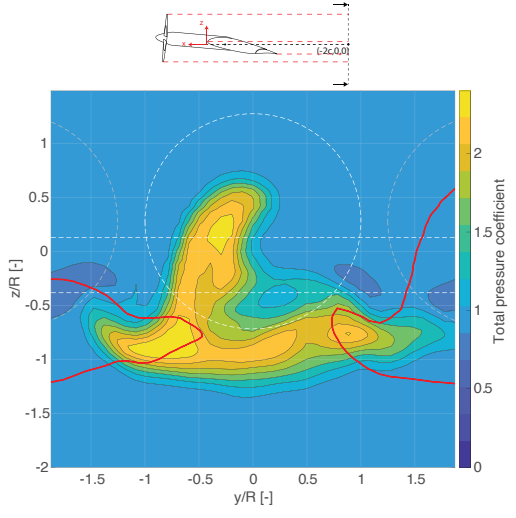


Figure 1 – Projected overlap of deformed slipstreams from adjacent propellers (in red) at high angles of attack. Modified from [5].

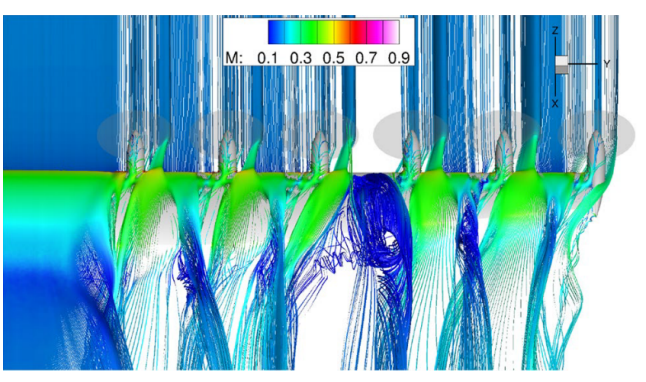


Figure 2 – Flow structures at interface of adjacent slipstreams in a distributed propeller configuration. From [7].

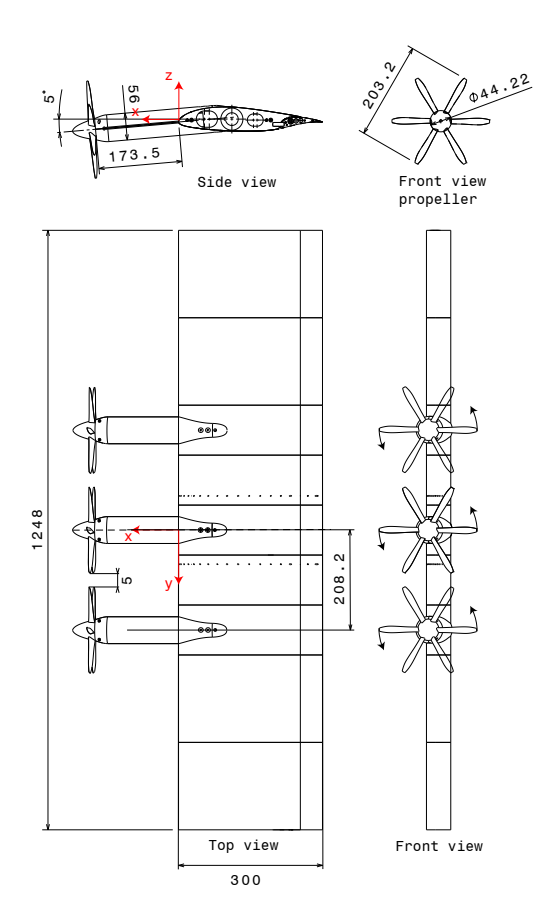
The purpose of this paper is therefore to offer a preliminary insight into the slipstream deformation in distributed propeller configurations and to identify key areas for future research. We present experimental measurements of the slipstream deformation of distributed propeller systems and compare this with results from a nearly identical experiment with only a single propeller installed, published previously in [5]. This allows us to directly compare between single and distributed propeller configurations. We analyse the difference in slipstream shape in the wake, as well as pressure distributions on the wing, between single and distributed propeller configuration. Additionally, we investigate the impact of blade phase angle on the slipstream deformation. In literature, phase control is recognised as a potential tool to reduce propeller noise [8], making it of interest how it may affect the propeller-wing interaction.

2. Experimental Setup

Experiments were performed in the Low Turbulence Tunnel (LTT) at the Delft University of Technology, a closed single-return tunnel with a turbulence level of approximately 0.015% at the testing velocity of $30 \ m/s$. The tunnel features interchangeable test sections with an octagonal cross-section. The test sections have a width of 1.8m, a height of 1.25m and length of 2.6m. The experimental setup of this experiment is identical to the setup used by Duivenvoorden et al. [5], with the exception of the number of propellers installed.

2.1 Model Geometry

The model consists of a straight, wall-to-wall wing with a chord length of 0.3m and span of 1.25m. A technical drawing of the model is presented in Fig. 3. The wing is fitted with three leading-edge propellers and has a single Fowler flap. Since no flap deflection was applied in this experiment, the flap gap was taped off to prevent bleed flow. The propellers used are the TUD-XPROP-S reference propellers [9], individually powered by electric motors. The propeller control system allows for different rotation directions and has accurate control over the phase of each propeller, meaning they can operate locked in phase at specific relative blade angles between the propellers. For all results shown in this document, the propellers are co-rotating in counter-clockwise direction when looking downstream. The definition of the blade phase angle is illustrated in Fig. 4.



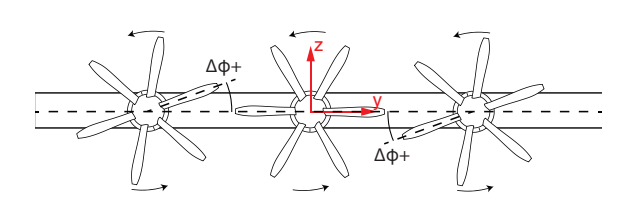


Figure 4 – Definition of the blade phase angle $\Delta \phi$.

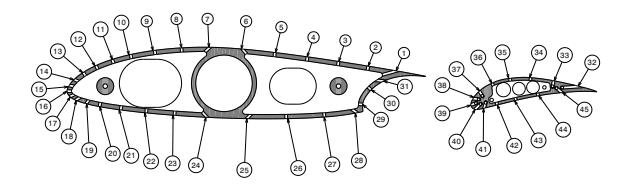


Figure 5 – Chordwise distribution of pressure taps on main element and flap.

Figure 3 – Technical drawing of wing model.

Dimensions in *mm*.

2.2 Measurement Techniques

A wake rake with total and static pressure probes was placed at a downstream location of x/c=-2, meaning the tips of the probes were positioned one chord-length from the wing trailing edge at $\alpha=0$ degrees. Figure 6 shows the dimensions and spacing of the probes. The wake rake was traversed in vertical and spanwise directions with respect to the test section. The measurement positions were chosen such that the entire slipstream is resolved with a resolution of at least $3\,mm$ in z-direction and a resolution of $10\,mm$ in y-direction.

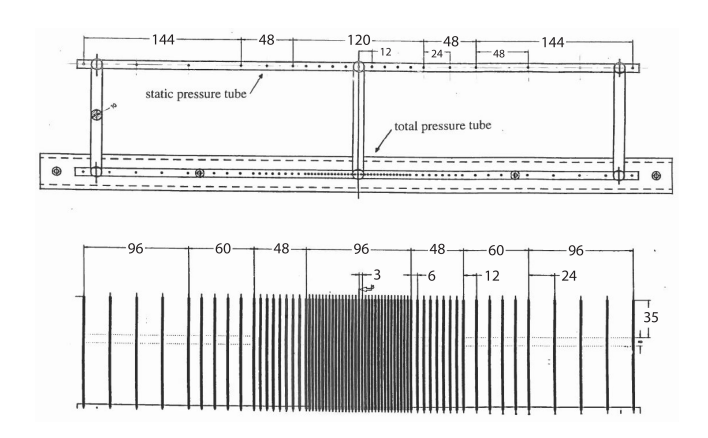


Figure 6 – Wake rake top and front view with spacing dimensions indicated in mm. Modified from [10]

The model also features two rows of pressure taps, the distribution of which is illustrated in Fig. 5. These are located at y/R = 0.7 on either side of the central nacelle, and are thus positioned within the slipstream of the center propeller. There was no telemetry on the propellers, apart from encoders to measure frequency and thermocouples to monitor motor temperature.

3. Results and Discussion

We compare wind-tunnel measurements of the distributed propeller configuration with those of the single propeller configuration from an earlier experimental campaign [5]. Additionally, we analyse the impact of blade phase angle on slipstream deformation and wing pressure distributions.

In the discussions in this paper, we use some common expressions to distinguish between various areas of the results. In the single propeller configuration, the positive y-coordinate is the upgoing blade side, while the downgoing blade side is in the negative y-direction. In the context of the distributed propeller case, we will always refer to different regions in the results relative to the central propeller, ensuring consistency with the single propeller configuration.

3.1 Single vs Multi-propeller slipstream

Figure 7 shows the total pressure coefficient (defined as $C_{p,t} = \frac{P_{rake} - P_{\infty}}{q_{\infty}}$) in the wake for both the single propeller (left) and distributed propeller (right) configurations at various angles of attack. The measurements highlight four primary differences: a reduction in slipstream deformation behind the central propeller, a shift in the nacelle vortex position, suppression of slipstream induced separation, and clear difference in deformation for the right-most propeller.

Slipstream deformation and distribution The maximum concentrations of $C_{p,t}$ in Fig. 7 are slightly higher in the distributed propeller configuration compared to the single propeller, but do not constitute a superposition of each propeller's contribution. Instead, the $C_{p,t}$ distribution remains more uniformly distributed and closer to its initial circular shape. At higher angles of attack (Figs. 7c through 7f), the reduction of slipstream deformation is even more pronounced. Particularly the upper half of the slipstream is much less concentrated on the downgoing blade side and the $C_{p,t}$ contours are overall more uniformly distributed.

Pressure distributions on the wing suggest that the wing itself is also more uniformly immersed in the slipstream. Figure 8 presents the pressure distributions of the single and distributed propeller configurations. The reader will notice fewer datapoints around x/c=0.7 for the distributed propulsion case, as these were taped off together with the flap gap. Dashed lines represent the upgoing blade side, while the solid lines are the downgoing blade side. The upgoing blade side pressure distributions closely match between the single and distributed propeller cases. On the downgoing blade side, however, suction on the upper surface is increased in the distributed propeller configuration. This suggests an overall reduction of slipstream deformation compared to the single propeller configuration.

The reduction of deformation also aligns with the theory of propeller-wing interaction mechanisms proposed by Felli [11], who attributes the deformation to the combination of vortex imaging effects and the spanwise pressure gradients. The presence of the adjacent slipstreams reduces the spanwise pressure gradient, thereby greatly reducing the spanwise deformation. Additionally, the vortex imaging effects of adjacent slipstreams will oppose each other at their interface, limiting the spanwise displacement.

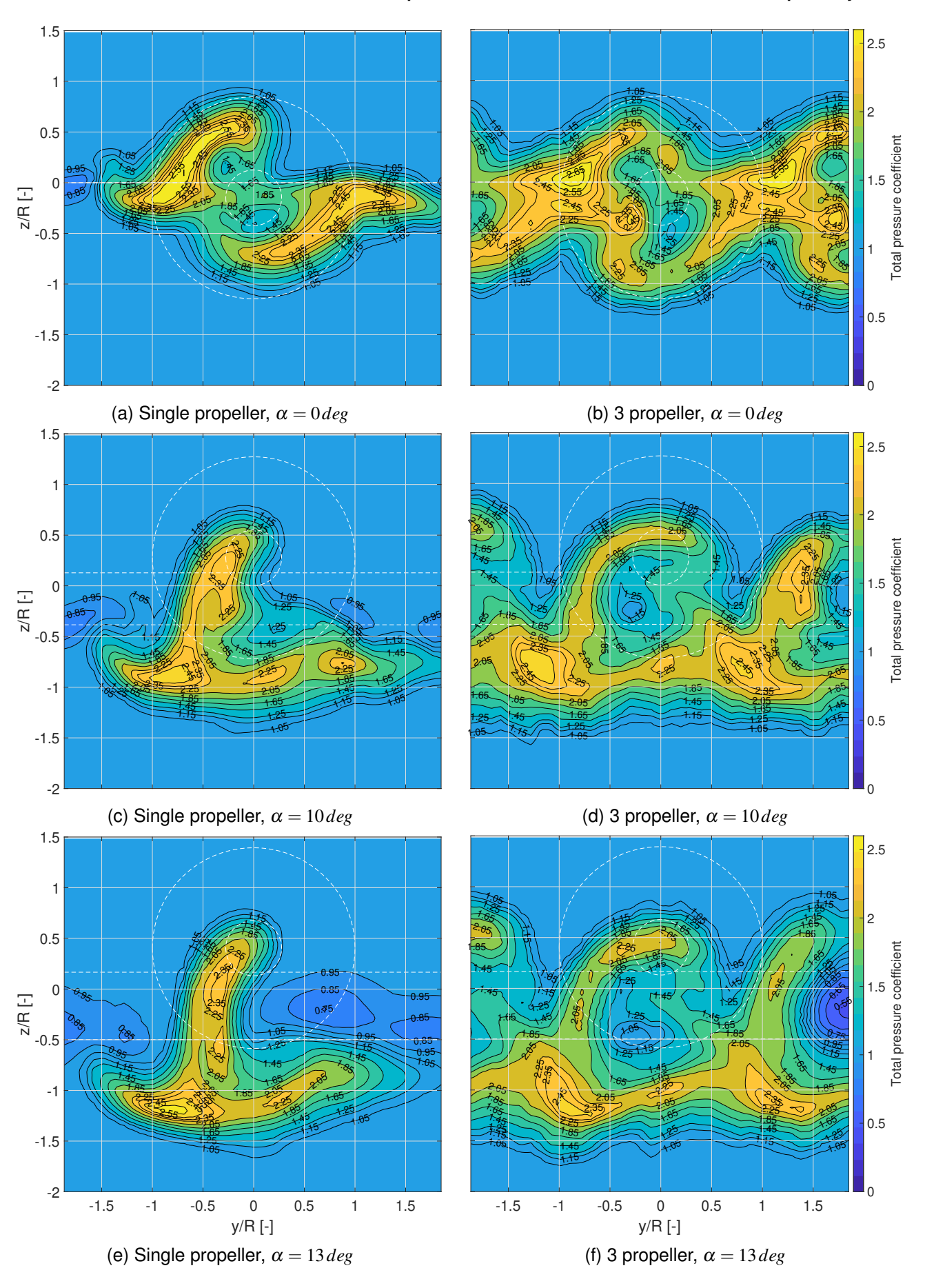


Figure 7 – Comparison of total pressure coefficient contours in the wake of a wing with single and distributed propellers. View in streamwise direction. Dashed lines indicate projections of the propeller, leading- and trailing-edge on the yz-plane. J=0.8, propellers out of phase. Modified from

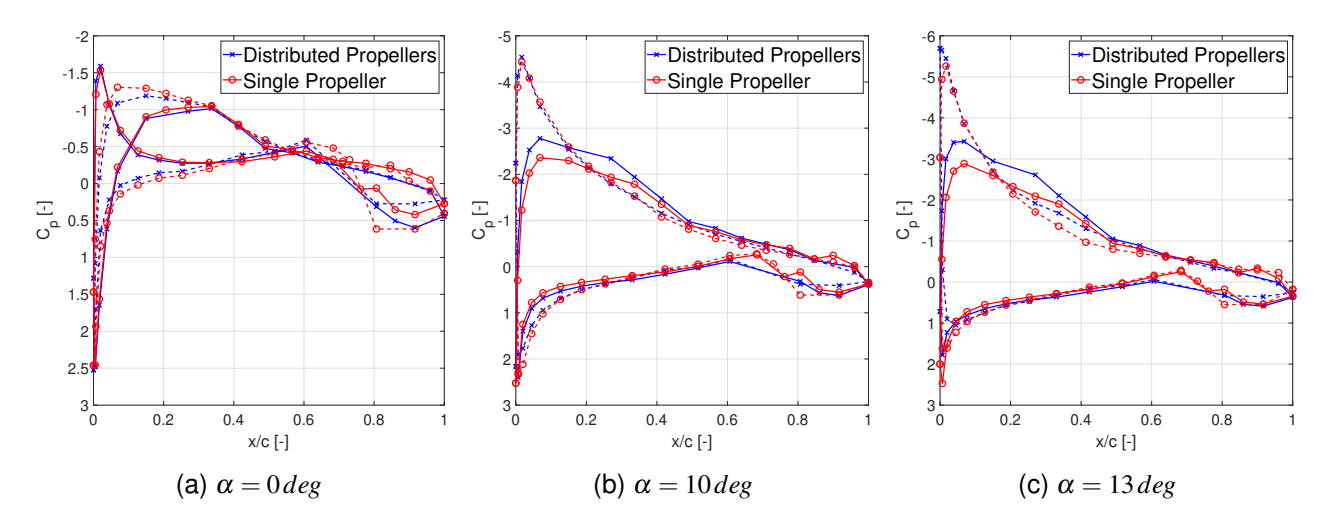


Figure 8 – Pressure distributions comparing single propeller with distributed propeller configuration for various angles of attack. Solid and dashed lines represent down-going and up-going blades sides, respectively.

The extent to which the slipstream deformation is reduced in distributed propeller configurations compared to the single propeller case warrants further investigation. The pressure distributions presented in Fig. 8 are local and the wing experiences strong spanwise variations under influence of the slipstream [5]. Slipstream deformation in the wing wake may dominate the resulting slipstream shape at the downstream station, while the slipstream shape on the wing itself may be similar between the distributed and single propeller configurations. The results presented here suggest, however, that a distributed propeller configuration would experience fewer negative effect of propeller-wing interaction in high-lift condition than the single propeller configuration.

Displacement of the nacelle vortex Figure 7 also reveals a low-pressure region at the center of the slipstream in the distributed propeller configuration, attributed to the nacelle vortex core. This low-pressure region is not as clearly defined in the single propeller measurements, except for a small area in Figure 7c. The limited spanwise resolution of the measurements and the relatively small size of the nacelle vortex core likely contribute to this discrepancy. However, numerical results for the single propeller configuration, published by Ribeiro et al. [6], confirm the presence of this region in the single propeller configuration, where it shifts spanwise to the upgoing blade side. In contrast, the distributed propeller measurements show the low-pressure region concentrated on the downgoing blade side. These observations indicate that distributed propeller configurations influence nacelle vortex development and spanwise displacement, warranting further investigation in future research.

Suppression of separation on the wing For a single propeller configuration at high angles of attack, the interaction of the propeller slipstream induces local areas of flow separation on the wing just outside of the slipstream [5]. In Figs. 7c and 7e, these can be seen as pockets of lower total pressure coefficient on the edge of the slipstream. For the distributed propeller configuration, these regions of separation are suppressed by the presence of adjacent slipstreams. This suppression is dependent on the propeller spacing, as shown by Bongen et al. [12] in a similar experiment.

In Fig. 7f, however, we observe a large region of separation next to the right-most slipstream. This region has a much lower total pressure coefficient than the separation regions measured in the single propeller configuration. This suggests that the separation induced by the slipstream-wing interaction may be stronger in the distributed propeller case, which would be critical to distributed propeller arrays that do not cover the entire wing. Whether this is the case, however, requires further investigation. In the experiments and simulations performed by Bongen et al. [12], similar separation regions occurred as a result of interactions with the wall junctions. Unfortunately, junction flows were not monitored in the present experiment.

We expect, however, that this region is a result of the slipstream-wing interaction and not just a wall-junction effect. In the single propeller experiment, wall junctions effects were monitored and the wall boundary layer was found to be small and of negligible effect on the flow at the centre of the wing. Local regions of separation outside the slipstream also occurred in that experiment, as a result of the slipstream-wing interaction. Furthermore, the spacing between the outermost propellers and the wind tunnel walls in this experiment are much larger than in the experiment by Bongen et al. [12], allowing the flow to stabilise in between the outer propellers and the wind tunnel walls.

Deformation of the outer slipstream The measurements of the distributed propeller configuration in finally show a clear difference in slipstream deformation for the outboard propellers. Although the individual slipstreams of the propellers are difficult to distinguish, it is evident that the slipstream of the right-most propeller experiences a different deformation as the central propeller's slipstream. In fact, the shape of the slipstream behind the right-most propeller in the distributed configuration is still reminiscent of the single propeller slipstream. This is illustrated in Fig. 9 by overlapping and aligning the single propeller contour lines on the distributed propeller measurements for $\alpha=10\,deg$. Compared to the single propeller configuration, however, it is not located directly behind the propeller but rather displaced significantly towards the centre propeller.

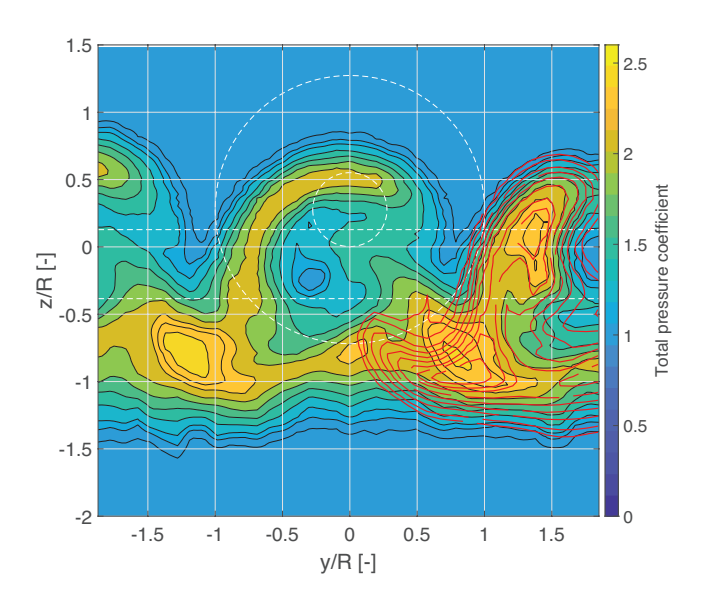


Figure 9 – Illustration of the similarity between the shape of the slipstream at the right-most propeller in the distributed propeller configuration and that of the single propeller case.

Interestingly, the left-most propeller slipstream shows much more similarity to the centre propeller. It is hard to fully judge based on the measurements of the present experiment, as the measurement area does not cover the propellers completely. Nonetheless, this could mean that rotation direction of the outer-most propellers of a finite distributed propeller array could have a critical role in the interaction with the wing.

The difference in slipstream deformation between the right-most and centre propeller signifies that the configuration is not representative of an infinite wing with an infinite array of propellers. This is an important consideration for experimental and numerical work on distributed propeller-wing interactions. Experiments in the field of distributed propellers are often conducted with a three-propeller setup (e.g., [13], [12]), while many numerical investigations apply a periodic boundary condition to a single propeller configuration (e.g., [14]). Crucially, although flow on the wing surface may look similar, the off-the-surface flow can behave significantly different.

3.2 Impact of phase control

Phase control is a recognised technique in literature as a potential method for reducing propeller noise [8]. In experiments of an isolated distributed propeller setup (i.e., without the wing) with the

same propellers, de Vries et al. [15] showed that the relative blade phase angle of the propellers has an effect on the interaction of the adjacent slipstreams at their interface. In the isolated case, this effect remained small and was ultimately insignificant. However, when these slipstreams interact with a lifting wing, the small deviations due to blade phase interactions could lead to significant differences in the slipstream deformation. We therefore measured the wake of the distributed propeller wing for several relative blade phase angles $\Delta \phi$. The results are shown in Figures 10 and 11, for $\alpha=0$ and $\alpha=8$ degrees respectively.

For low angle of attack, the impact of the blade phase angle remains small. Some variations occur on the upper right and lower left portions of the distributions. For $\alpha=8$ degrees, the impact of $\Delta\phi$ is more significant. As $\Delta\phi$ increases, the total pressure distributions in the central portion of the slipstream (around y/R=0) gradually change shape and become more concentrated. Past $\Delta\phi\approx30\,deg$, the changes revert gradually. Considering the propellers have six blades, the effects of $\Delta\phi$ will repeat every 60 degrees and the relative distance between tip vortices of adjacent propellers is mirrored around $\Delta\phi=30\,deg$. Figures 10 and 11 do show this periodic behaviour, although it is not mirrored about $\Delta\phi=30\,deg$ exactly.

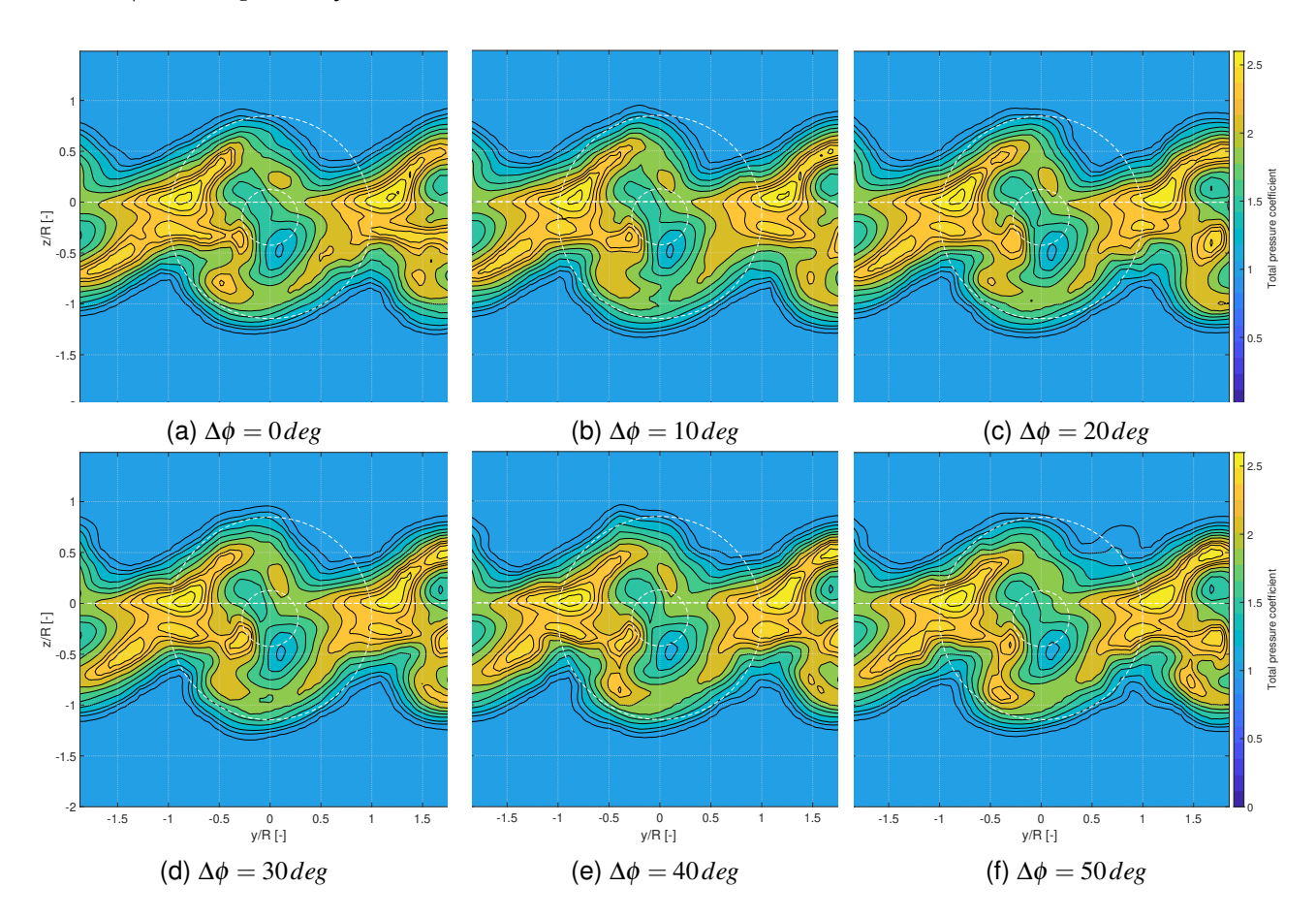


Figure 10 – Contours of $C_{p,t}$ for distributed propellers at varying $\Delta \phi$. $\alpha = 0 deg$.

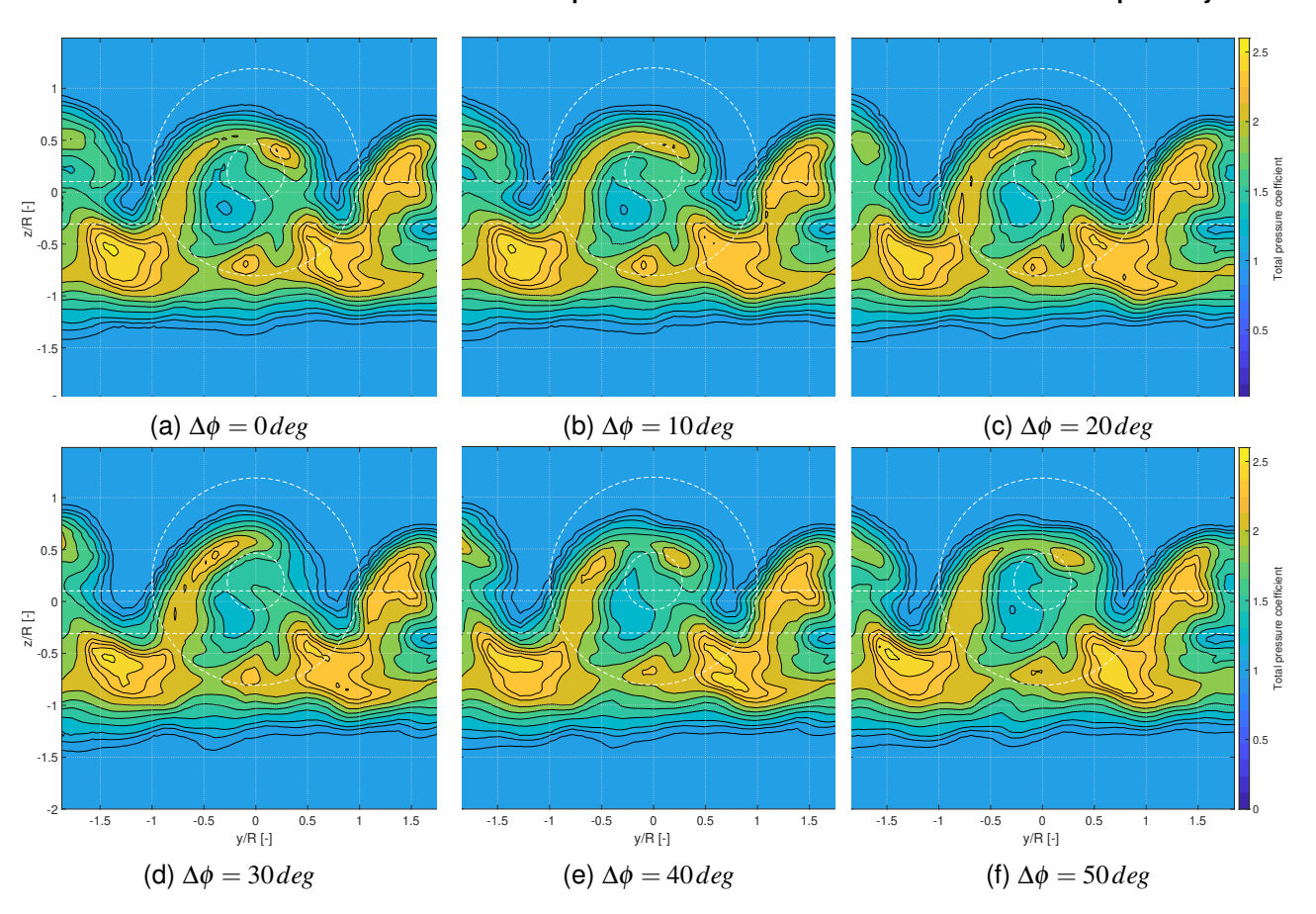


Figure 11 – Contours of $C_{p,t}$ for distributed propellers at varying $\Delta \phi$. $\alpha = 8 deg$.

At low angle of attack, $\Delta\phi$ mostly affects the distribution at the slipstream interfaces, while for higher angles this changes to the central portion of the slipstream. This is better visualised in Fig. 12. It shows a contour map of the maximum deviation from the mean across all measured values of $\Delta\phi$ for the data presented in Figures 10 and 11. For $\alpha=0\,deg$, deviations are concentrated around the edge of the slipstream. They mostly remain within 10-15% of the mean value, with some local outlier regions. For $\alpha=8\,deg$, however, deviations are clearly concentrated on the upper half of the slipstream, on the upgoing blade side. The $\Delta\phi$ clearly affects the development of that part of the slipstream for high angles of attack. Interestingly, the slipstream behind the right-most propeller is hardly affected by changes to $\Delta\phi$, as illustrated by Fig. 11. This is not the case for the low angle of attack results.

The pressures on the wing are virtually unaffected by the changes in $\Delta\phi$, as shown by Fig. 13. It shows the deviation from the mean pressure distribution as a result of $\Delta\phi$. Clearly, the blade phase angle does not affect the local pressure distributions significantly. Unfortunately we cannot definitively conclude that the impact of blade phase angle on the slipstream development is restricted to the wake region, as the pressure taps are located quite far from the location where the slipstreams interact. In that region, local pressures may be affected more significantly, which will require additional measurements to resolve.

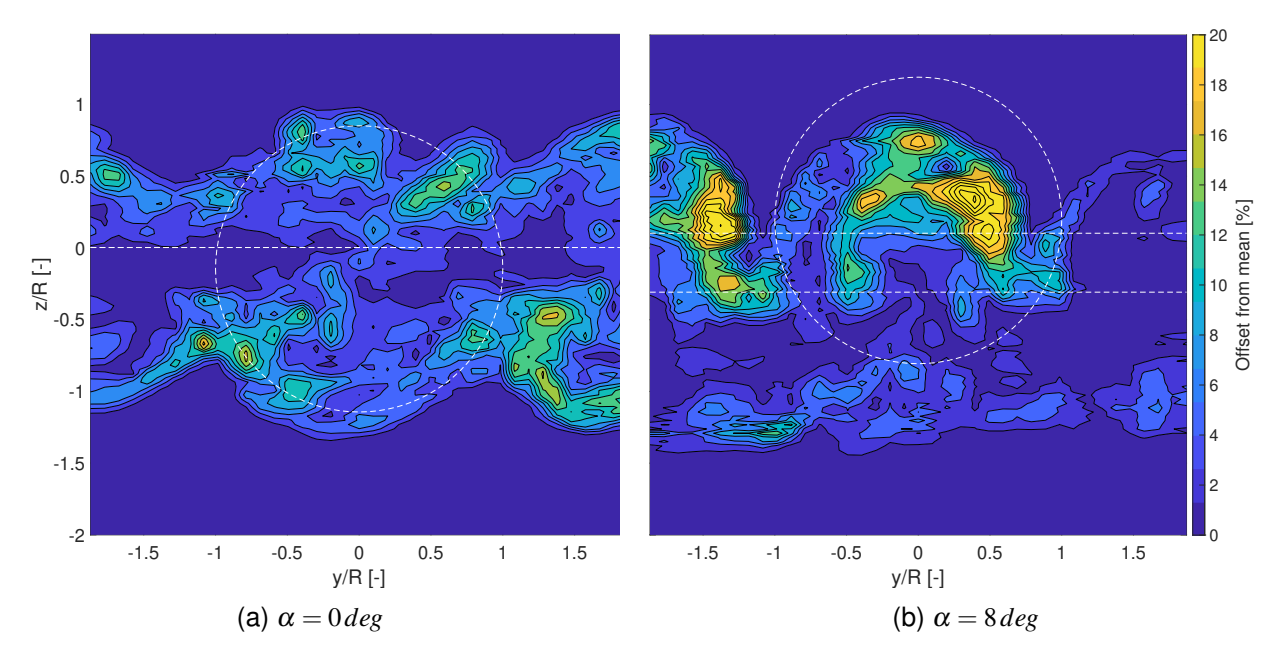


Figure 12 – Contour plots showing the maximum deviation from the mean as a result of changing blade phase angle.

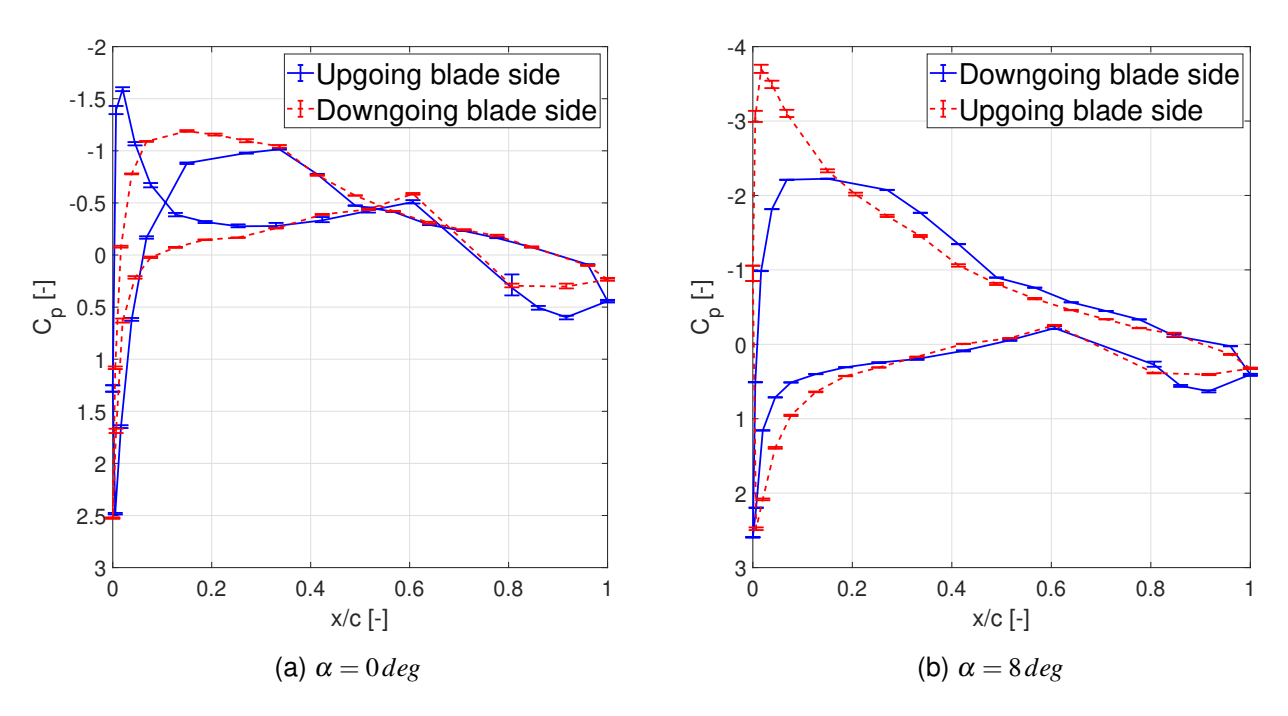


Figure 13 – Pressure distributions on the wing with variability due to variations in blade phase angle shown as error bars.

4. Conclusion and Recommendations

In this paper, we have shown wind tunnel measurements of the slipstream deformation in the wake of an installed distributed propeller configuration, along with pressure distributions on the wing. These measurements include both low and high angles of attack, but without flap deflections. We compared these measurements with previous experiments of the same setup with a single propeller installed.

Overall, we have identified several key differences between single and distributed installed propeller configurations in terms of propeller-wing aerodynamic interaction. Furthermore, we assessed the impact of phase control on the slipstream development of a distributed propeller configuration. To-

gether, these lead to various phenomena in distributed propeller-wing interaction that warrant further investigation:

- Compared to the single propeller configuration, the slipstream remains more uniformly distributed, indicating more uniform immersion of the wing in the slipstream. This may be particularly significant for multi-section wings and lead to better high-lift performance compared to single propeller configurations.
- Phase control has a clear effect on the slipstream deformation in the wake at higher angles of attack, specifically on the upgoing blade side. Further study is required to determine whether the local wing performance is equally affected, which would be a critical consideration when utilising phase control to suppress propeller noise.
- The separation induced by a single propeller slipstream at high angles of attack is suppressed by adjacent propeller slipstreams. However, the induced separation at the end of a distributed propeller array may be stronger as a result.
- The wake of the distributed propeller configuration shows very different deformations for the
 centre propeller and the right-most propeller, meaning the centre propeller performance does
 not represent an infinite propeller array. This needs to be considered when setting up experiments to provide experimental validation data for numerical simulations of installed distributed
 propeller systems.

5. Contact Author Email Address

The contact author for this document is R.R. (Ramon) Duivenvoorden, MSc. r.r.duivenvoorden@tudelft.nl

6. Copyright Statement

The authors confirm that they, and/or their company or organization, hold copyright on all of the original material included in this paper. The authors also confirm that they have obtained permission, from the copyright holder of any third party material included in this paper, to publish it as part of their paper. The authors confirm that they give permission, or have obtained permission from the copyright holder of this paper, for the publication and distribution of this paper as part of the ICAS proceedings or as individual off-prints from the proceedings.

References

- [1] Jeffrey K. Viken, Sally Viken, Karen A. Deere, and Melissa Carter. Design of the Cruise and Flap Airfoil for the X-57 Maxwell Distributed Electric Propulsion Aircraft. In *35th AIAA Applied Aerodynamics Conference*, number June, pages 1–41, Reston, Virginia, jun 2017. American Institute of Aeronautics and Astronautics. ISBN 978-1-62410-501-2. doi: 10.2514/6.2017-3922.
- [2] Reynard de Vries, Nando van Arnhem, Tomas Sinnige, Roelof Vos, and Leo L.M. Veldhuis. Aerodynamic interaction between propellers of a distributed-propulsion system in forward flight. *Aerospace Science and Technology*, 118:107009, 2021. ISSN 12709638. doi: 10.1016/j.ast. 2021.107009.
- [3] Ingemar Samuelsson. Experimental Investigation of Low Speed Model Propeller Slipstream Aerodynamic Characteristics Including Flow Field Surveys and Nacelle/Wing Static Pressure Measurements. In 17th Congress of the International Council of the Aeronautical Sciences, pages 17–84, Stockholm, Sweden, 1990. International Council of the Aeronautical Sciences.
- [4] L.L.M. Veldhuis. *Propeller wing aerodynamic interference*. Phd dissertation, Delft University of Technology, 2005.
- [5] Ramon Duivenvoorden, Noah Suard, Tomas Sinnige, and Leo L. Veldhuis. Experimental Investigation of Aerodynamic Interactions of a Wing with Deployed Fowler Flap under Influence of a Propeller Slipstream. In AIAA AVIATION 2022 Forum, pages 1–19, Reston, Virginia,

- jun 2022. American Institute of Aeronautics and Astronautics. ISBN 978-1-62410-635-4. doi: 10.2514/6.2022-3216.
- [6] Andre F. Ribeiro, Ramon Duivenvoorden, and Diogo Martins. High-Fidelity Simulations of Propeller-Wing Interactions in High-Lift Conditions. In AIAA AVIATION 2023 Forum, number June, pages 1–16, San Diego, CA, jun 2023. American Institute of Aeronautics and Astronautics. ISBN 978-1-62410-704-7. doi: 10.2514/6.2023-3541.
- [7] Dennis Keller. Towards higher aerodynamic efficiency of propeller-driven aircraft with distributed propulsion. CEAS Aeronautical Journal, 12(4):777–791, nov 2021. ISSN 1869-5582. doi: 10.1007/s13272-021-00535-5.
- [8] Kyle A. Pascioni, Stephen A. Rizzi, and Noah H. Schiller. Noise reduction potential of phase control for distributed propulsion vehicles. In *AIAA Scitech 2019 Forum*, number January, pages 1–16, 2019. ISBN 9781624105784. doi: 10.2514/6.2019-1069.
- [9] Nando van Arnhem, Reynard de Vries, Tomas Sinnige, Roelof Vos, Georg Eitelberg, and Leo L. M. Veldhuis. Engineering Method to Estimate the Blade Loading of Propellers in Nonuniform Flow. AIAA Journal, 58(12):5332–5346, dec 2020. ISSN 0001-1452. doi: 10.2514/1.J059485.
- [10] L.M.M. Boermans and P.B. Rutten. Two-dimensional aerodynamic characteristics of airfoil NLF-MOD22 with fowler flap. Technical report, Delft University of Technology, Delft, 1995.
- [11] M. Felli. Underlying mechanisms of propeller wake interaction with a wing. *Journal of Fluid Mechanics*, 908:A10, feb 2021. ISSN 0022-1120. doi: 10.1017/jfm.2020.792.
- [12] Dustin Bongen, Mário Firnhaber Beckers, Michael Schollenberger, Dominique P. Bergmann, Thorsten Lutz, Alex Gothow, Mahmod Saeed, Julien Weiss, Andreas Bardenhagen, and Rolf Radespiel. Simulation of a Distributed Propulsion System in a Wind Tunnel. In AIAA AVIATION 2022 Forum, pages 1–18, Chicago, Illinois, jun 2022. American Institute of Aeronautics and Astronautics. ISBN 978-1-62410-635-4. doi: 10.2514/6.2022-3818.
- [13] Devansh R. Agrawal, Faisal Asad, Blake Berk, Trevor Long, Jackson Lubin, Christopher Courtin, Mark Drela, R John Hansman, and Jacqueline Thomas. Wind Tunnel Testing of a Blown Flap Wing. In AIAA Aviation Forum, number June, pages 1–20, Dallas, Texas, 2019. American Institute of Aeronautics and Astronautics. doi: 10.2514/6.2019-3170.
- [14] Mário Firnhaber Beckers, Michael Schollenberger, Thorsten Lutz, Dustin Bongen, Rolf Radespiel, Juan L. Florenciano, and David E. Funes-Sebastian. Numerical Investigation of High-Lift Propeller Positions for a Distributed Propulsion System. *Journal of Aircraft*, 60(4):995–1006, 2023. ISSN 15333868. doi: 10.2514/1.C037248.
- [15] Reynard de Vries, Nando van Arnhem, Francesco Avallone, Daniele Ragni, Roelof Vos, Georg Eitelberg, and Leo L. Veldhuis. Aerodynamic Interaction Between an Over-the-Wing Propeller and the Wing Boundary-Layer in Adverse Pressure Gradients. In AIAA Aviation Forum, number June, pages 1–19, Dallas, Texas, 2019. American Institute of Aeronautics and Astronautics. doi: 10.2514/6.2019-3035.